Noname manuscript No.
(will be inserted by the editor)

Real-Time Trajectory Generation Trading-Off Control Effort and Flight Time for Hovering Vehicles

Weihong Yuan · Luis Rodrigues

Received: date / Accepted: date

Abstract Real-time onboard flight trajectory generation is of great importance for all kinds of vehicles. This paper addresses trajectory generation for a trade-off between minimum control effort and flight time. The problem is formulated using a point mass model with three forces acting on the body, namely thrust, drag and gravity, which is a good model for quadrotor unmanned aerial vehicles (UAVs). An analytical solution is provided to generate the optimal trajectory for arbitrary feasible boundary conditions. An approximate solution is also derived for long-haul flights, which can reduce the computational time. A characteristic parameter is proposed to decide whether the flight is long haul or not so as to choose the type of solution: the analytic or the approximate solution. The algorithm can compute the trajectory either for a given flight time, or for a free time. Moreover, the approach is extended to respect peak velocity constraints. Examples show the applicability of the proposed method.

Keywords optimal trajectory generation · minimum control effort · real-time onboard computation

1 Introduction

This paper deals with vehicles that can hover in 3D space, such as quadrotor UAVs. Europe has adopted the Flightpath 2050 challenge demanding that by 2050, 90 percent of all the travelers are able to complete their journey door-to-door within four hours. The vision also states that "the transport system must be resilient against disruptive events and must be capable of automatically and dynamically reconfiguring the journey within the network if disruption occurs"[1]. A similar concept took shape earlier in the USA named SATS (Small Aircraft Transportation System), aiming at dealing with the saturation of existing transportation systems [2]. For these aircraft, it is essential to be able to generate or regenerate an optimal flight trajectory in real-time.

Many trajectory generation methods have been developed, such as the sampling-based approach [3], artificial heuristic approach [4], geometry-based approach [5], BADA model-based approach [6] and dynamic programming [7], to name a few. To achieve a certain level of abstraction, so as to provide beneficial robustness in flight trajectory tracking, it is favorable to have a double layered system, namely a Flight Management System (FMS) as the upper level and a Flight Control System (FCS) as the lower level. A FMS generates waypoints or continuous guidance and feeds them into the FCS, whose task is to control the aircraft to track the trajectory [8].

Applying optimal control theory to flight trajectory planning dates back to the 1950s, starting with fixed-wing aircraft and spacecraft orbits. The authors in [9] investigated the fuel-optimal trajectory and summarized existing dynamic models to formulate the problem. Reference [10] studied the minimal direct operating cost (DOC) trajectory, which is the sum of fuel cost and time-related costs. References [8,11] solved the DOC-optimal airspeed profiles for climb, cruise, and descent phases for jet and all-electric aircraft, respectively. The articles [12,13] studied the time-optimal trajectory for quadrotors. Feasible ranges of the control inputs were studied in [12]. Reference [14] tackled the minimal acceleration trajectory for quadrotors in a 2D vertical

Weihong Yuan · Luis Rodrigues
Concordia University, Montreal, Canada

plane. The work presented in [15] was on snap-optimal trajectory. The research published in [16] studied the minimal control effort trajectory in the vertical plane with 1D drag. The study was performed for zero boundary conditions only taking the pitch angle and thrust as control inputs. It was claimed in the paper that a completely analytical solution was not possible. The authors in [17] investigated a similar problem even though it was interpreted as the energy-optimal trajectory. A second order drag model was considered and some constraints on states and control inputs were incorporated. However, the problem was solved in 1D space. Unfortunately, the 3D trajectory would not simply be the combination of the three decoupled 1D trajectories. Similar to [16], only the optimal control law was obtained instead of an explicit solution of the optimal trajectory. Reference [18] solved numerically the optimal trajectory for a quadrotor UAV with 16 states. The objective of our paper is to solve the optimal trajectory by trading-off control effort and flight time. The benefits of the result are threefold, 1) it implies a potential longer lifetime of the actuators and less maintenance cost, 2) it implies less energy consumption since control effort is directly related to energy consumption, 3) it might require less space and weight for the aircraft at an early design stage.

Compared to the previous work in the literature, the main contributions of this paper are as follows:
a) Analytically solving for a minimal control effort trajectory for arbitrary boundary conditions, considering linear drag. The approach can find the trajectory for either a fixed time or a free time.
b) Proposing an approximate solution for long haul flights to reduce the computational time. A characteristic parameter is proposed to decide whether to use the analytical solution or the approximation.
c) Extending the approach to verify peak velocity constraints.

The structure of this paper is as follows. Section 2 presents the problem formulation and the detailed solution of the optimal trajectory generation problem, including the optimal trajectory and the optimal flight time. Simulation results are presented in section 3. Concluding remarks are stated in section 4.

2 Problem Formulation and Methodology

UAVs that can hover in 3D space have three types of forces, namely gravity, thrust and drag. Since this paper offers a conceptual framework for optimal trajectory generation, other models can also be studied with the methodology developed in this section.

2.1 Problem Description

Assume that an aircraft at current state x_0 receives a command to reach the destination x_f at time t_f. The problem to be solved in this paper is to generate the trajectory between x_0 and x_f that optimizes a functional that trades off control effort and flight time. This optimal trajectory is to be found for both a fixed and a free flight time.

To formulate and solve this problem we make the following assumptions:

1. The vehicle conserves its mass, or mass depletion is sufficiently slow. Electric vehicles naturally fall into this condition.

2. The drag is linear in the velocity written as

$$D = -k_d v \tag{1}$$

where D is drag, v is velocity, and k_d is assumed to be a constant for a given flight. For lower Reynold's numbers ($Re < 10^3$), this is a reasonable assumption called linear Stokes drag [23,24]. For higher Reynold's numbers, it is just an approximation and valid only within a small range in the neighborhood of the target velocity.

3. The wind effect and air density variation are ignored.

4. The only forces acting on the aircraft are thrust, drag and weight.

2.2 Problem Formulation

Define the state vector $x = [p_1, p_2, p_3, v_1, v_2, v_3]^T$, where p is the vector of position coordinates, v is the vector of velocity coordinates. The system dynamics are

$$\begin{bmatrix} \dot{p_1} \\ \dot{p_2} \\ \dot{p_3} \\ \dot{v_1} \\ \dot{v_2} \\ \dot{v_3} \end{bmatrix} = \begin{bmatrix} 0\,0\,0\,1\,0\,0 \\ 0\,0\,0\,0\,1\,0 \\ 0\,0\,0\,0\,0\,1 \\ 0\,0\,0\,0\,0\,0 \\ 0\,0\,0\,0\,0\,0 \\ 0\,0\,0\,0\,0\,0 \end{bmatrix} \begin{bmatrix} p_1 \\ p_2 \\ p_3 \\ v_1 \\ v_2 \\ v_3 \end{bmatrix} + \begin{bmatrix} 0\,0\,0 \\ 0\,0\,0 \\ 0\,0\,0 \\ 1\,0\,0 \\ 0\,1\,0 \\ 0\,0\,1 \end{bmatrix} \begin{bmatrix} a_1 \\ a_2 \\ a_3 \end{bmatrix} \tag{2}$$

$$\begin{bmatrix} T_1 \\ T_2 \\ T_3 \end{bmatrix} = m \left(\begin{bmatrix} a_1 \\ a_2 \\ a_3 \end{bmatrix} + \begin{bmatrix} 0 \\ 0 \\ g \end{bmatrix} \right) + k_d \begin{bmatrix} v_1 \\ v_2 \\ v_3 \end{bmatrix} \tag{3}$$

The optimal control problem is

$$\begin{aligned} J = \min \quad & \int_0^{t_f} \frac{1}{2} T^T T + C_I dt \\ s.t. \quad & (2), (3) \\ & x(t_0) = x_0 \\ & x_f \text{ given} \end{aligned} \tag{4}$$

where C_I is the ratio of cost of time and cost of control effort. Define

$$\lambda = \frac{\partial J(x)}{\partial x} \tag{5}$$

$$H = L(x,T) + \lambda^T f(x,T) \tag{6}$$

where $L(x,T) = \frac{1}{2} T^T T + C_I$ and $f(x,T)$ is defined in (2).The terms L, H are the running cost and the Hamiltonian, respectively. A detailed interpretation of analytical mechanics using the Lagrangian and the Hamiltonian can be found in [19]. The Pontryagin Maximum Principle (PMP) is used to find the optimal control. Further details on PMP and calculus of variations can be obtained in references [21,22]. The necessary conditions for a minimizer are

$$\frac{\partial H^*}{\partial T} = 0 \tag{7}$$

$$\frac{\partial H^*}{\partial x} = -\dot{\lambda} \tag{8}$$

2.3 3D trajectory solution

Theorem 1: The optimal flight trajectory is

$$\begin{bmatrix} p_1 \\ p_2 \\ p_3 \end{bmatrix} = \begin{bmatrix} -\frac{C_1}{k_d^2} t - \frac{C_4}{2k_d^2} e^{\frac{k_d}{m} t} - \frac{C_7 m}{k_d} e^{-\frac{k_d}{m} t} + C_{10} \\ -\frac{C_2}{k_d^2} t - \frac{C_5}{2k_d^2} e^{\frac{k_d}{m} t} - \frac{C_8 m}{k_d} e^{-\frac{k_d}{m} t} + C_{11} \\ -\frac{C_3}{k_d^2} t - \frac{C_6}{2k_d^2} e^{\frac{k_d}{m} t} - \frac{C_9 m}{k_d} e^{-\frac{k_d}{m} t} + C_{12} \end{bmatrix} \tag{9}$$

where p_i is the position, k_d is the drag coefficient, m is the mass, and

$$\begin{bmatrix} C_i \\ C_{i+3} \\ C_{i+6} \\ C_{i+9} \end{bmatrix} = \begin{bmatrix} -v_{0i} k_d^2 - \frac{k_d}{2m} C_{i+3} + C_{i+6} k_d^2 \\ \frac{(p_{fi} - p_{0i}) + (v_{fi} - v_{0i}) \frac{m}{k_d} - v_{0i} t_f - \frac{\left(v_{fi} - v_{0i}\right) t_f e^{\frac{k_d}{m} t_f}}{e^{\frac{k_d}{m} t_f} - 1}}{\frac{t_f}{2mk_d}\left(e^{\frac{k_d}{m} t_f} + 1\right) - \frac{1}{k_d^2}\left(e^{\frac{k_d}{m} t_f} - 1\right)} \\ -\frac{(v_{fi} - v_{0i}) e^{\frac{k_d}{m} t_f}}{e^{\frac{k_d}{m} t_f} - 1} - \frac{e^{\frac{k_d}{m} t_f}}{2mk_d} C_{i+3} \\ p_{0i} + \frac{1}{2k_d^2} C_{i+3} + \frac{m}{k_d} C_{i+6} \end{bmatrix} \tag{10}$$

for $i = 1, 2, 3$.

Proof: The Hamiltonian of (4) is,

$$\begin{aligned} H &= \frac{1}{2} T^2 + \lambda_1 \dot{p_1} + \lambda_2 \dot{p_2} + \lambda_3 \dot{p_3} + \lambda_4 \dot{v}_1 + \lambda_5 \dot{v}_2 + \lambda_6 \dot{v}_3 + C_I \\ &= \frac{1}{2}(T_1^2 + T_2^2 + T_3^2) + \lambda_1 v_1 + \lambda_2 v_2 + \lambda_3 v_3 + C_I + \\ &\frac{\lambda_4}{m}(T_1 - k_d v_1) + \frac{\lambda_5}{m}(T_2 - k_d v_2) + \frac{\lambda_6}{m}(T_3 - k_d v_3 - mg) \end{aligned} \tag{11}$$

From (7),

$$\frac{\partial H^*}{\partial T} = \begin{bmatrix} T_1 \\ T_2 \\ T_3 \end{bmatrix} + \frac{1}{m} \begin{bmatrix} \lambda_4 \\ \lambda_5 \\ \lambda_6 \end{bmatrix} = \begin{bmatrix} 0 \\ 0 \\ 0 \end{bmatrix} \tag{12}$$

$$T^* = \frac{1}{m}[-\lambda_4, -\lambda_5, -\lambda_6]^T \tag{13}$$

$$\begin{aligned} H^* = &-\frac{1}{2m^2}(\lambda_4^2 + \lambda_5^2 + \lambda_6^2) + \lambda_1 v_1 + \lambda_2 v_2 + \lambda_3 v_3 \\ &- \frac{k_d}{m}(\lambda_4 v_1 + \lambda_5 v_2 + \lambda_6 v_3) - \lambda_6 g + C_I \end{aligned} \tag{14}$$

From (8),

$$\frac{\partial H^*}{\partial p} = \begin{bmatrix} 0 \\ 0 \\ 0 \end{bmatrix} = \begin{bmatrix} -\dot{\lambda}_1 \\ -\dot{\lambda}_2 \\ -\dot{\lambda}_3 \end{bmatrix}, \frac{\partial H^*}{\partial v} = \begin{bmatrix} \lambda_1 - \frac{k_d}{m}\lambda_4 \\ \lambda_2 - \frac{k_d}{m}\lambda_5 \\ \lambda_3 - \frac{k_d}{m}\lambda_6 \end{bmatrix} = \begin{bmatrix} -\dot{\lambda}_4 \\ -\dot{\lambda}_5 \\ -\dot{\lambda}_6 \end{bmatrix} \tag{15}$$

$$[\lambda_1, \lambda_2, \lambda_3]^T = [C_1, C_2, \bar{C}_3]^T \tag{16}$$

$$\begin{bmatrix} \lambda_4 \\ \lambda_5 \\ \lambda_6 \end{bmatrix} = \begin{bmatrix} \frac{C_1 m}{k_d} + C_4 e^{\frac{k_d}{m} t} \\ \frac{C_2 m}{k_d} + C_5 e^{\frac{k_d}{m} t} \\ \frac{\bar{C}_3 m}{k_d} + C_6 e^{\frac{k_d}{m} t} \end{bmatrix} = -m \begin{bmatrix} T_1 \\ T_2 \\ T_3 \end{bmatrix} \tag{17}$$

From (3),

$$\dot{v} = a = \frac{1}{m} \begin{bmatrix} -\frac{C_1}{k_d} - \frac{C_4}{m} e^{\frac{k_d}{m} t} - k_d v_1 \\ -\frac{C_2}{k_d} - \frac{C_5}{m} e^{\frac{k_d}{m} t} - k_d v_2 \\ -\frac{\bar{C}_3}{k_d} - \frac{C_6}{m} e^{\frac{k_d}{m} t} - k_d v_3 - mg \end{bmatrix} \tag{18}$$

Define C_3 as,

$$C_3 = \bar{C}_3 + mgk_d \tag{19}$$

Integrating (18) and using (19) yields,

$$v = \begin{bmatrix} -\frac{C_1}{k_d^2} - \frac{C_4}{2mk_d} e^{\frac{k_d}{m} t} + C_7 e^{-\frac{k_d}{m} t} \\ -\frac{C_2}{k_d^2} - \frac{C_5}{2mk_d} e^{\frac{k_d}{m} t} + C_8 e^{-\frac{k_d}{m} t} \\ -\frac{C_3}{k_d^2} - \frac{C_6}{2mk_d} e^{\frac{k_d}{m} t} + C_9 e^{-\frac{k_d}{m} t} \end{bmatrix} \tag{20}$$

Integrating (20), (9) is obtained.
The boundary conditions are,

$$\begin{bmatrix} p(0) \\ v(0) \end{bmatrix} = x_0, \begin{bmatrix} p(t_f) \\ v(t_f) \end{bmatrix} = x_f \tag{21}$$

After solving (21) using (9), (20), we get (10). We observe that the denominator of C_{i+3} will never be zero. To show this, let $Q = \frac{k_d t_f}{m} > 0$, then the denominator equal to zero is equivalent to $Q(e^Q+1)-2(e^Q-1)=0$. Since the derivative of the left-hand-side is $(Q-1)e^Q+1$. It is monotonically increasing, and when $Q=0$, $(Q-1)e^Q+1=0$. Therefore, $Q(e^Q+1)-2(e^Q-1) > 0(e^0+1)-2(e^0-1)=0$. Q.E.D.

Theorem 2: The optimal cost for a given flight time t_f is

$$J^* = \left(\frac{1}{2}m^2g^2 + C_I\right)t_f - mg\left[\frac{C_3}{k_d}t_f + \frac{C_6}{k_d}\left(E(t_f)-1\right)\right] + \sum_{i=1}^{3}\left[\frac{C_i^2}{2k_d^2}t_f + \frac{C_{i+3}^2}{4k_d m}\left(E(2t_f)-1\right) + \frac{C_i C_{i+3}}{k_d^2}\left(E(t_f)-1\right)\right] \tag{22}$$

where $E(t) = e^{\frac{k_d}{m}t}$.

Proof: From (17), (19), we get

$$\begin{bmatrix} T_1 \\ T_2 \\ T_3 \end{bmatrix} = \begin{bmatrix} -\frac{C_1}{k_d} - \frac{C_4}{m}E(t) \\ -\frac{C_2}{k_d} - \frac{C_5}{m}E(t) \\ -\frac{C_3}{k_d} - \frac{C_6}{m}E(t) + mg \end{bmatrix} \tag{23}$$

By plugging (23) into the cost function in (4) and integrating, expression (22) is obtained. Q.E.D.

Approximation 1: For longer t_f, i.e. $\frac{k_d}{m}t_f > 5$, an approximate solution is

$$p_i = p_{0i} + (v_{fi} + \frac{k_d}{m}lf_i)t - lf_i E(t-t_f) + \left[\frac{m}{k_d}(v_{fi}-v_{0i}) + lf_i\right]\left(E(-t)-1\right) \tag{24}$$

where $i = 1, 2, 3$, and

$$lf = \frac{(p_f - p_0) + \frac{(v_f - v_0)}{k_d}m - v_f t_f}{\frac{k_d}{m}t_f - 2} = -\frac{mv_f}{k_d} + \frac{(p_f - p_0) - \frac{m}{k_d}(v_f + v_0)}{\frac{k_d}{m}t_f - 2} \tag{25}$$

$$J^* = \left(\frac{1}{2}m^2g^2 + C_I + mgk_d v_{f3} + gk_d^2 lf_3\right)t_f - 2mgk_d lf_3 + \sum_{i=1}^{3}\left[\frac{k_d^2}{2}t_f\left(v_{fi} + \frac{k_d}{m}lf_i\right)^2 + \frac{k_d^3}{m}lf_i^2 - 2k_d^2 lf_i\left(v_{fi} + \frac{k_d}{m}lf_i\right)\right] \tag{26}$$

In fact, when $\frac{k_d}{m}t_f > 5$, the following hold,

$$E(t_f) > 100 \gg 1 \tag{27}$$

$$E(t_f) \pm 1 \approx E(t_f) \tag{28}$$

One can then approximate C_{i+3}, for $i = 1, 2, 3$, as

$$C_{i+3} = \frac{(p_{fi} - p_{0i}) + (v_{fi} - v_{0i})\frac{m}{k_d} - v_{fi}t_f}{\left(\frac{t_f}{2mk_d} - \frac{1}{k_d^2}\right)E(t_f)} = \frac{2k_d^2}{E(t_f)}lf_i \tag{29}$$

Then (10) becomes

$$\begin{bmatrix} C_i \\ C_{i+3} \\ C_{i+6} \\ C_{i+9} \end{bmatrix} = \begin{bmatrix} -k_d^2(v_{fi} + \frac{k_d}{m}lf_i) \\ \frac{2k_d^2}{E(t_f)}lf_i \\ -(v_{fi} - v_{0i}) - \frac{k_d}{m}lf_i \\ p_{0i} - \frac{m}{k_d}(v_{fi} - v_{0i}) - lf_i \end{bmatrix} \tag{30}$$

Using (30) in (9) yields (24). Plugging (30) into (22), (26) is obtained. Accordingly, the new velocity profile is

$$v_i = (v_{fi} + \frac{k_d}{m}lf_i) - \frac{k_d}{m}lf_i E(t-t_f) - \left[(v_{fi} - v_{0i}) + \frac{k_d}{m}lf_i\right]E(-t) \tag{31}$$

Remark 1: $E(t_f)$ and lf are a scalar and a vector, respectively, for a given set of boundary conditions and flight time t_f.

Remark 2: The condition for the approximation can be loosen to $\frac{k_d}{m}t_f > 3$, so as to obtain an approximation error $\frac{E(t_f)}{E(t_f)-1} \approx 1.0524$, meaning about 5% of relative error for this approximation when $\frac{k_d}{m}t_f = 3$. The approximate trajectory will be shown in the next section. When $\frac{k_d}{m}t_f < 3$, Theorem 1 and 2 have to be applied. The optimal flight time t_f is sought with numerical methods for 1D optimization problems, such as Golden Section Search, or Successive Parabolic Interpolation [25], because there are over 20 terms in the cost function, which makes the gradient based optimization too expensive to analyze and solve. For $\frac{k_d}{m}t_f > 3$, the optimal t_f can be obtained with the following result.

Theorem 3: For the long haul flight approximation, the optimal flight time t_f is unique when the control input in unbounded, and can be written as

$$t_f = \frac{m}{k_d}\left(2 + \frac{k_d^2}{m}\sqrt{\frac{|(p_f - p_0) - \frac{m}{k_d}(v_f + v_0)|^2}{m^2g^2 + 2C_I}}\right) \tag{32}$$

Proof: For each fixed final time t_f, an optimal cost is obtained in (22) or (26), which can be regarded as a

mapping from t_f to J^*, i.e. $J^* = J^*(t_f)$. The optimal t_f satisfies $\frac{\partial J^*}{\partial t_f} = 0$. Rewrite the term lf as

$$lf = -\frac{mv_f}{k_d} + \frac{(p_f - p_0) - \frac{m}{k_d}(v_f + v_0)}{\frac{k_d}{m}t_f - 2} = A + \frac{B}{Z-2} \tag{33}$$

where A, B are two constant vectors, that are independent of t_f, and $Z = \frac{k_d}{m}t_f$. Then

$$v_f + \frac{k_d}{m}lf = \frac{k_d}{m}\frac{B}{(Z-2)} \tag{34}$$

Using this relation and recalling (26) and (33) yields

$$\frac{\partial J^*}{\partial t_f} = \frac{k_d}{m}\frac{\partial J^*}{\partial Z} \tag{35}$$

$$\frac{\partial J^*}{\partial Z} = \sum_{i=1}^{3} -\frac{k_d^3}{2m}\frac{B_i^2}{(Z-2)^2} + \left(\frac{m^2g^2}{2} + C_I\right)\frac{m}{k_d} \tag{36}$$

Since $Z > 3$, it is obvious that equation (36) has one and only one admissible root. Therefore, J^* has one and only one minimizer on the right half plane. Set

$$\frac{\partial J^*}{\partial t_f} = 0 \tag{37}$$

Solving (37) for t_f yields

$$t_f = \frac{m}{k_d}\left(2 + \frac{k_d^2}{m}\sqrt{\frac{\sum_{i=1}^{3} B_i^2}{m^2g^2 + 2C_I}}\right) \tag{38}$$

Therefore, (32) is proven. Q.E.D.

We define the characteristic parameter

$$CV = \frac{3C_D}{4}\frac{\rho_{air}}{\rho_{craft}}\frac{dist}{l} \tag{39}$$

where C_D is the drag coefficient, ρ_{air}, ρ_{craft} is air density and effective aircraft density, respectively, $dist$ is the flight distance, and l is the aircraft length.
This parameter determines whether to use the theoretical solution ($CV < 3$) or the approximation ($CV \geq 3$).

Considering the smallest outer sphere surrounding the hovering aircraft, the diameter of the sphere equals to the aircraft length l. The volume of the sphere is $\frac{1}{6}\pi l^3 = \frac{2}{3}Al$, where A is the effective area of the outer sphere surrounding the aircraft defined as $A = \frac{1}{4}\pi l^2$. Define the effective aircraft density ρ_{craft} as mass divided by the volume of the sphere. Choosing k_d with average velocity magnitude v_{avg}, we expand the terms as

$$\frac{k_d}{m}t_f = \frac{\frac{1}{2}C_D\rho_{air}Av_{avg}t_f}{\rho_{craft}A\frac{2}{3}l} = \frac{3C_D}{4}\frac{\rho_{air}}{\rho_{craft}}\frac{dist}{l} \tag{40}$$

Note that C_D is a function of the Reynold's number, which is defined as

$$Re = \frac{\rho_{air}}{\mu}v_{avg}l \tag{41}$$

For a given aircraft, $\frac{k_d}{m}t_f$ is a function of the flying environment (atmosphere), estimated average speed, and flight distance. Therefore, it can be regarded as a characteristic parameter for the flight trajectory.

Theorem 4: There is at most one peak velocity during flight.

Proof: R is the square of the velocity magnitude, and can be obtained from (20) as

$$R = |v(t)|^2 = \sum_{i=1}^{3}\left[\frac{C_i^2}{k_d^4} + \frac{C_{i+3}^2}{4m^2k_d^2}E(2t) + C_{i+6}^2E(-2t) + \frac{C_iC_{i+3}}{mk_d^3}E(t) - \frac{2C_iC_{i+6}}{k_d^2}E(-t) - \frac{C_{i+3}C_{i+6}}{mk_d}\right] \tag{42}$$

Define,

$$\begin{aligned} a &= \sum_{i=1}^{3}\frac{C_{i+3}^2}{4m^2k_d^2} \geq 0 \\ b &= \sum_{i=1}^{3} C_{i+6}^2 \geq 0 \\ c &= \sum_{i=1}^{3}\frac{C_iC_{i+3}}{mk_d^3} \\ d &= \sum_{i=1}^{3} -\frac{2C_iC_{i+6}}{k_d^2} \\ e &= \sum_{i=1}^{3}\frac{C_i^2}{k_d^4} - \frac{C_{i+3}C_{i+6}}{mk_d} \end{aligned} \tag{43}$$

Then we have,

$$\begin{aligned} &R = aW^2 + \frac{b}{W^2} + cW + \frac{d}{W} + e \\ &W = E(t) \in [1, E(t_f)] \end{aligned} \tag{44}$$

The function R is differentiable on t since it is the summation of differentiable functions. Additionally, W is monotonic on t without sign change, and is never zero. Define the function Q as

$$\begin{aligned} Q &= \frac{\partial R}{\partial W}W^3 = (2aW - \frac{2b}{W^3} + c - \frac{d}{W^2})W^3 \\ &= \left(2aW^4 + cW^3 - dW - 2b\right) \end{aligned} \tag{45}$$

Let W_m be the zero-crossing point of the function Q from positive to negative values within the interval $W \in$

$[1, E(t_f)]$, which corresponds to the maximizer of the function R. Therefore, the peak value of R during the flight is found as

$$max(R) = max\left(R(1), R(E(t_f)), R(W_m)\right) \tag{46}$$

The following two cases are possible:
1. $a = 0$.
Then we have $C_{i+3} = 0, i \in \{1, 2, 3\}$, so that $c = 0$, and then $Q = -dW - 2b$. Since $-2b \leq 0$, there is no zero-crossing point of function Q from positive to negative values within the interval $W \in [1, E(t_f)]$. An example is shown in Fig. 1a. The single peak velocity will therefore occur at either $W = 1$ or $W = E(t_f)$.
2. $a \neq 0$.
The function Q is a quartic function. Only when Q has four distinct real roots, there are two zero-crossing points in the direction from positive to negative values. An example is shown in Fig. 1d. Otherwise, there is at most one zero-crossing point from positive to negative values, for example in Fig. 1b and Fig. 1c. Assume there are two maximizers in $W > 0$. Note that we must have $Q(0) > 0$ because Q decreases on the left of the first root. Since $Q(W = 0) = -2b \leq 0$, we obtain a contradiction. Therefore, there must be at most one maximizer in $W > 0$. Q.E.D.

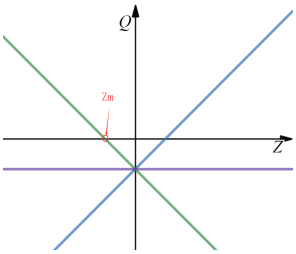

(a) Function Q for case 1

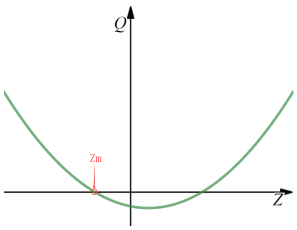

(b) Function Q for case 2, two simple roots

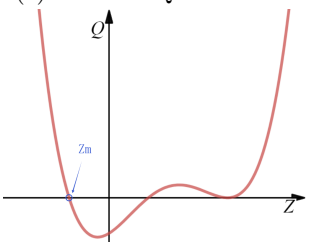

(c) Function R for case 3, two simple roots and one double root

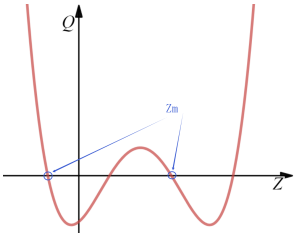

(d) Function R for case 4, four distinct roots

Fig. 1: Curves of function R for all cases

Remark 3: A proposed solution to find the feasible flight time t_f which verifies the peak velocity constraint is to find the shortest time such that $max(R) \leq V_{max}^2$.

3 Simulation Results

Two cases are studied in this section, one being a smaller electric rotorcraft, the other being a bigger manned electric helicopter. Their k_d is calculated with a coefficient of drag C_D chosen from reference [23] assuming that they are rough spherical objects and with v_{avg} obtained by dividing distance with time. In Fig. 4, the dotted line is the trajectory from Theorem 1, while the crossed line is the approximate solution from Approximation 1.

3.1 Case 1: Smaller rotorcraft

Let $x_0 = [-1.5, 0, 1, 1, 0, -1]^T$ and $x_f = [10, 2, 5, 0, 2, 0]^T$. Taking the DJI Phantom 4 Pro [27] as an example, $m = 1.388kg, l = 0.35m, C_D = 0.3, C_I = 10$. The air density $\rho_{air} = 1.225kg/m^3$ is chosen from reference [26] at sea level. The parameter $CV = 0.15716 \ll 3$. In this case, Theorem 1 and 2 have to be used. The optimal flight time is $t_f = 2.6813s$. Fig. 2 shows the optimal 3D trajectory and the corresponding velocity, acceleration, thrust, position and cost over time. The final position error is $1.819e^{-12}m$, i.e., it is a factor of $1.4742e^{-13}$ of the whole distance of $12.3390m$, merely because of roundoff error. The velocity stays well within range under the upper limit of $20m/s$. The velocity peak and valley of acceleration in the middle are caused by the relatively low boundary velocities. The thrust takes values between $13 \sim 23N$. The final cost is 355.8. The Pareto trade-off curve of this flight is depicted in Fig. 3, which illustrates the tradeoff between the flight time and control effort, and indicates that a larger C_I leads to a shorter flight time and higher control effort.

3.2 Case 2: Larger manned helicopter

Let $x_0 = [-1.5, 0, 10, 30, 5, 3]^T$ and $x_f = [17810, 26370, 3645, 4, 32, 0]^T$. Taking the Sikorsky Firefly [28] as an example, $m = 930kg, l = 2.54m, C_D = 0.3, C_I = 10$. The air density $\rho_{air} = 1.0251kg/m^3$ is chosen from reference [26] at the middle altitude of the two boundary points. The parameter $CV = 26.8335 > 3$, so Approximation 1, Theorem 3 and 4 can be used. The optimal flight time is $t_f = 736.3338s$. Fig. 4 shows the optimal 3D trajectory and the corresponding velocity, acceleration, thrust, position and cost over time. The lines of the exact solution and the approximate one match well with each other, meaning that the approximate solution can represent the exact solution with minor errors. The calculation is much faster for the approximate solution. The final position error is $1.99e^{-09}m$,

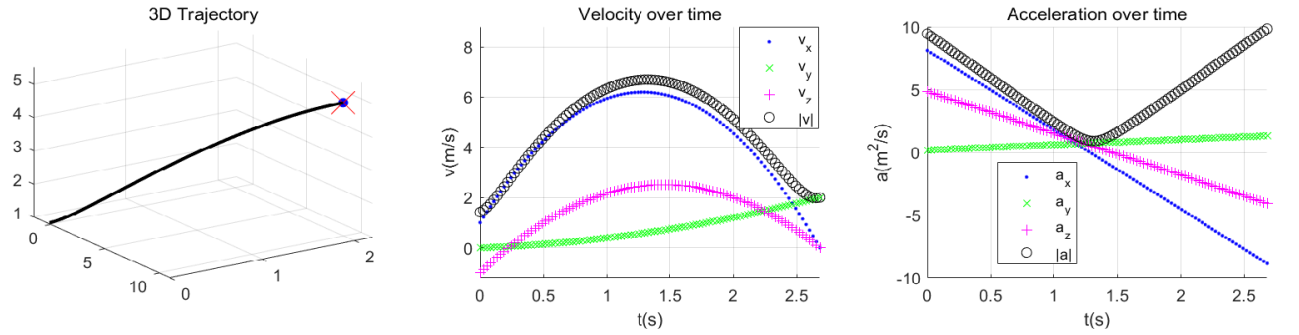

Fig. 2: Optimal trajectory for smaller rotorcraft.

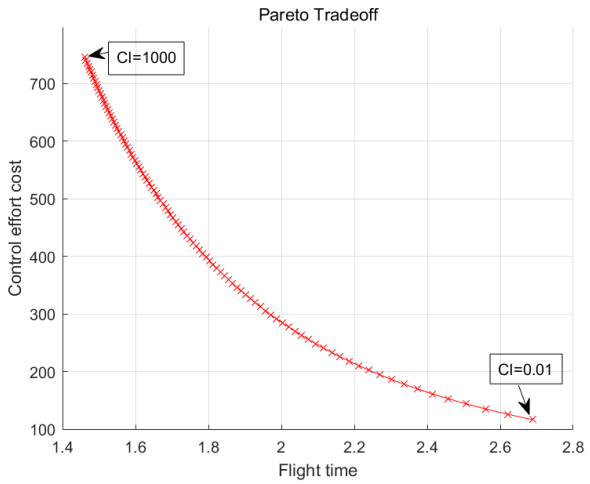

Fig. 3: Pareto trade-off of CI

i.e., it is a factor of $6.2269e^{-14}$ of the whole distance of $32028.73m$. The acceleration plot shows that the trajectory has a peak value of less than $1.5m/s^2$. The thrust magnitude is slowly varying and the cost is approximately linear as a function of time. For this long haul example, a cruise-like phase appears during the flight.

4 Conclusions

In this paper, we presented a complete analytical solution of the optimal trajectory generation problem trading-off control effort and flight time. The approach allows arbitrary boundary conditions, and both fixed and free flight times. An approximate solution for long haul flights was derived so as to reduce the computational time. A characteristic term was proposed to determine whether to use the analytical solution or the approximation. The method was extended to respect peak velocity constraints.

Acknowledgements The authors would like to acknowledge Marinvent Corporation and the Mathematics of Information Technology and Complex Systems (MITACS) for funding this research.

References

1. S. Kallas et al, "Flightpath 2050 Europe's Vision for Aviation," Report of the High Level Group on Aviation Research, European Commission, Brussels, Belgium, Report no.EUR, vol. 98, 2011.
2. S. A. Viken, F. M. Brooks and S. C. Johnson, "Overview of the small aircraft transportation system project four enabling operating capabilities," J. Aircr., vol. 43, (6), pp. 1602-1612, 2006.
3. P. Pharpatara, B. Hérissé and Y. Bestaoui, "3-D Trajectory Planning of Aerial Vehicles Using RRT*," in IEEE Transactions on Control Systems Technology, vol. 25, no. 3, pp. 1116-1123, May 2017.
4. R. S. F. Patrón and R. M. Botez, "Flight trajectory optimization through genetic algorithms coupling vertical and lateral profiles," in ASME 2014 International Mechanical Engineering Congress and Exposition, 2014, .
5. I. Lugo-Cárdenas, G. Flores, S. Salazar and R. Lozano, "Dubins path generation for a fixed wing UAV," 2014 International Conference on Unmanned Aircraft Systems (ICUAS), Orlando, FL, 2014, pp. 339-346.
6. E. S. Palacios and M. A. Johnson, "4D BADA-based Trajectory Generator and 3D Guidance Algorithm," NASA, CA, USA, 2013. Accessed on: Feb., 12, 2019. [Online].
7. S. Kumakshev and A. Shmatkov, "Flight trajectory optimization without decomposition into separate stages," in IOP Conference Series: Materials Science and Engineering, 2018, .
8. J. Villarroel, "An Optimal Control Framework for Flight Management Systems.", Concordia University, 16 February 2015.
9. R. L. Schultz and N. R. Zagalsky, "Aircraft performance optimization." J. Aircr., vol. 9, (2), pp. 108-114, 1972.
10. J. A. Sorensen, S. A. Morello and H. Erzberger, "Application of trajectory optimization principles to minimize aircraft operating costs," 1979 18th IEEE Conference on Decision and Control including the Symposium on Adaptive Processes, Fort Lauderdale, FL, USA, 1979, pp. 415-421.
11. M. Kaptsov and L. Rodrigues, "Flight management systems for all-electric aircraft," 2017 IEEE Conference on Control Technology and Applications (CCTA), Mauna Lani, HI, 2017, pp. 2126-2131.

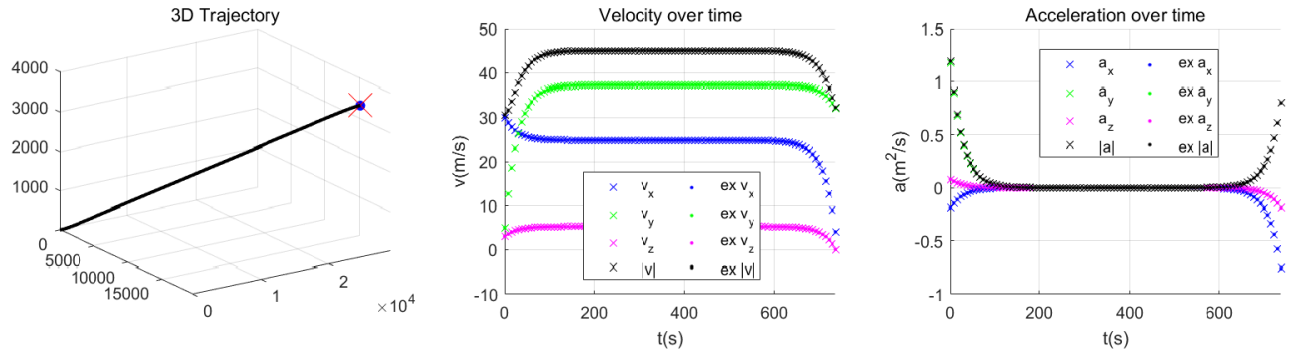

Fig. 4: Optimal trajectory for manned helicopter.

12. M. Hehn and R. D'Andrea, "Quadrocopter Trajectory Generation and Control," IFAC Proceedings Volumes, vol. 44, (1), pp. 1485-1491, 2011.
13. R. Ritz et al, "Quadrocopter performance benchmarking using optimal control," 2011 IEEE/RSJ International Conference on Intelligent Robots and Systems, San Francisco, CA, 2011, pp. 5179-5186.
14. B. Carvalho, M. D. Perna and L. Rodrigues, "Real-time optimal trajectory generation for a quadrotor uav on the longitudinal plane," in European Control Conference, Cyprus, June 2018, pp. 3132-3136.
15. D. Mellinger and V. Kumar, "Minimum snap trajectory generation and control for quadrotors," 2011 IEEE International Conference on Robotics and Automation, Shanghai, 2011, pp. 2520-2525.
16. B. Carvalho and L. Rodrigues, "Optimal Longitudinal Trajectory Planning for a Quadrotor UAV Including Viscous Drag Effects." , in European Control Conference, Naples, June 2019, accepted.
17. A. Taitler et al, "Combined time and energy optimal trajectory planning with quadratic drag for mixed discrete-continuous task planning," Optimization, vol. 68, (1), pp. 125-143, 2019.
18. F. Morbidi, R. Cano and D. Lara, "Minimum-energy path generation for a quadrotor UAV," in 2016 IEEE International Conference on Robotics and Automation (ICRA), 2016,.
19. P. Hamill, A Student's Guide to Lagrangians and Hamiltonians. 2014.
20. D. P. Bertsekas et al, Dynamic Programming and Optimal Control. 20051(3).
21. D. Liberzon, Calculus of Variations and Optimal Control Theory: A Concise Introduction. 2011.
22. L. S. Pontryagin, Mathematical Theory of Optimal Processes. 2018.
23. J. P. Owen and W. S. Ryu, "The effects of linear and quadratic drag on falling spheres: an undergraduate laboratory," European Journal of Physics, vol. 26, (6), pp. 1085, 2005.
24. R. Barati and S. Neyshabouri, "Comment on "Summary of frictional drag coefficient relationships for spheres Evolving solution strategies applied to an old problem," Chemical Engineering Science, vol. 181, pp. 90-91, 2018.
25. P. Jarratt, "An iterative method for locating turning points," The Computer Journal, vol. 10, (1), pp. 82-84, 1967.
26. U. NOAA and U. A. Force, US Standard Atmosphere, 1976, 1976.
27. DJI, "Phantom 4 Pro," Retrieved from https://www.dji.com/ca/phantom-4-pro/info, 2018.
28. Electric VTOL News, "Sikorsky Firefly," Retrieved from http://evtol.news/aircraft/sikorsky-firefly/, 2018.